

# Influence of the excited states on the electron-energy distribution function in low-pressure microwave argon plasmas

A. Yanguas-Gil,\* J. Cotrino, and A. R. González-Elipe

*Instituto de Ciencias de Materiales de Sevilla and Departamento de Física Atómica, Molecular y Nuclear and Química Inorgánica (CSIC, Universidad de Sevilla), Sevilla, Spain*

(Received 31 January 2005; published 7 July 2005)

In this work the influence of the excited states on the electron-energy distribution function has been determined for an argon microwave discharge at low pressure. A collisional-radiative model of argon has been developed taking into account the most recent experimental and theoretical values of argon-electron-impact excitation cross sections. The model has been solved along with the electron Boltzmann equation in order to study the influence of the inelastic collisions from the argon excited states on the electron-energy distribution function. Results show that under certain conditions the excited states can play an important role in determining the shape of the distribution function and the mean kinetic energy of the electrons, depleting the high-energy tail due to inelastic processes from the excited states, especially from the  $4s$  excited configuration. It has been found that from the populations of the excited states an excitation temperature can be defined. This excitation temperature, which can be experimentally determined by optical emission spectroscopy, is lower than the electron kinetic temperature obtained from the electron-energy distribution function.

DOI: [10.1103/PhysRevE.72.016401](https://doi.org/10.1103/PhysRevE.72.016401)

PACS number(s): 52.80.Pi, 52.20.Fs, 52.25.Dg

## I. INTRODUCTION

In the last 20 years there has been an increasing interest in plasma modeling due to the number of applications of plasma discharges, ranging from thin-film deposition to plasma sterilisation [1–3]. Although gas mixtures used in the literature vary enormously, argon has become one of the most common gases, along with oxygen, being usually used as a carrier gas in the different mixtures.

The purpose of the present work is to study the effect of argon-excited states on the electron-energy distribution function. Although the populations of the excited states are generally much lower than the gas density, the electrons involved in the inelastic collisions associated with these levels are far less energetic than those needed for inelastic processes from the ground state. Compared to the 11 eV of the energy gap between the argon ground state and the  $4s$  excited configuration, transitions between the  $4s$  and the  $4p$  or  $5p$  excited configurations have an energy threshold of a few electronvolts.

The influence of these processes on the electron-energy distribution function (EEDF) has been taken into account by developing an extensive argon collisional-radiative (CR) model. This model is based on a set of electron-impact cross sections in which the more recent experimental results have been used. The collisional-radiative model has been self-consistently solved along with the electron Boltzmann equation in the classical two-term expansion approximation.

Several argon collisional-radiative models, such as those of Bretagne *et al.* [4], Vlcek [5], and the later modifications of Bogaerts *et al.* [6] and Bultel *et al.* [7], have been published in the last decades. However, most of these models present cross sections which are based on analytical expres-

sions which fit the experimental data normally from well before the 1990s. In the present work the whole argon cross-section set has been updated using when possible cross sections based on experimental results.

This paper is organized as follows: in Sec. II the argon CR model is described and the choice of the different cross sections is discussed and compared with previous models. Section III is devoted to the coupling of the argon CR model and the electron Boltzmann equation. Calculations are presented for an argon microwave plasma in Sec. IV. In Secs. V and VI the results obtained are discussed and summarized.

## II. ARGON COLLISIONAL-RADIATIVE MODEL

The model proposed in the present work considers 32 individual and effective levels ranging from the argon neutral ground state to the argon singly ionized state at 15.76 eV. All the argon-excited states with energies below 15 eV have been gathered in 30 real and lumped levels, as described in Table I. The degeneracies of the effective levels, formed by more than one individual excited state, have been obtained as the sum of those of the individual states and the energy of the lumped levels calculated as the mean of those of the real levels, weighted by their degeneracies. The levels configurations have been named using the  $j$ - $K$  coupling notation convention, the primed configurations being for those levels with core angular momentum of  $j_c=1/2$ , whereas unprimed configurations correspond to  $j_c=3/2$ . The argon-excited states above 15 eV have not been taken into account due to the intercombination of states from different configurations that takes place at these energies. However, the influence of the excited states optically connected with argon ground state has been considered indirectly through radiative cascades.

Two kind of processes are considered in the present work: electron-impact collisions and radiative processes. Although the influence of excitation and ionization through heavy par-

\*Electronic address: [angel.yanguas@icmse.csic.es](mailto:angel.yanguas@icmse.csic.es)

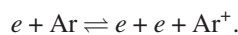
TABLE I. Summary of the argon-excited levels considered.

Number	Configuration	Deg.	Energy (eV)
0	$3s^2p^6$	1	0
1	$4s[3/2]_2, ^3P_2$	5	11.548
2	$4s[3/2]_1, ^3P_1$	3	11.623
3	$4s'[1/2]_0, ^3P_0$	1	11.723
4	$4s'[1/2]_1, ^1P_1$	3	11.828
5	$4p[1/2]_1$	3	12.907
6	$4p[5/2]_3$	7	13.076
7	$4p[5/2]_2$	5	13.095
8	$4p[3/2]_1$	3	13.153
9	$4p[3/2]_2$	5	13.172
10	$4p[1/2]_0$	1	13.273
11	$4p'[3/2]_1$	3	13.283
12	$4p'[3/2]_2$	5	13.302
13	$4p'[1/2]_1$	3	13.328
14	$4p'[1/2]_0$	1	13.480
15	$3d5s$	48	14.019
16	$3d'5s'$	24	14.246
17	$5p[1/2]_0$	3	14.464
18	$5p[5/2]_3$	7	14.499
19	$5p[5/2]_2$	5	14.506
20	$5p[3/2]_1$	3	14.525
21	$5p[3/2]_2$	5	14.529
22	$5p[1/2]_0$	1	14.564
23	$5p'[3/2]_1$	3	14.681
24	$5p'[1/2]_1$	3	14.687
25	$5p'[3/2]_2$	5	14.688
26	$5p'[1/2]_0$	1	14.738
27	$4d$	40	14.780
28	$6s$	8	14.842
29	$4f$	56	14.906
30	$4d'$	20	14.967
31	$3s^2p^5$	6	15.76

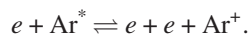
ticle's impact may be important at higher pressures, having an important role as a electron-loss pathway in argon atmospheric discharges [8], it can be in principle neglected in low-pressure, low-temperature discharges and will not be considered in present work.

Electron-impact inelastic processes:

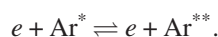
(i) Electron-impact ionization and recombination to the ground state:



(ii) Electron-impact ionization and recombination to an excited state:



(iii) Electron-impact excitation and deexcitation:



The electron-impact processes are characterized by a rate coefficient  $K_{ij}$ . For a direct transition ( $\varepsilon_j > \varepsilon_i$ ) this coefficient can be expressed as

$$K_{ij} = \sqrt{\frac{2}{m}} \int_{\varepsilon_{ij}}^{\infty} \sigma_{ij}(\varepsilon) \varepsilon F(\varepsilon) d\varepsilon,$$

where  $\sigma_{ij}$  is the associated electron-impact cross section,  $F(\varepsilon)$  the EEDF normalized so that  $\int \varepsilon^{1/2} F(\varepsilon) d\varepsilon = 1$ ,  $\varepsilon_{ij}$  is the threshold energy, and  $m$  is the electron mass.

The rate coefficients for the inverse processes can be expressed by applying the detailed balance principle [5]:

$$K_{ji} = \frac{g_i}{g_j} \sqrt{\frac{2}{m}} \int_{\varepsilon_{ij}}^{\infty} \sigma_{ij}(\varepsilon) \varepsilon F(\varepsilon - \varepsilon_{ij}) d\varepsilon$$

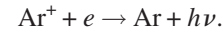
and

$$K_{ci} = \frac{g_i}{g_e g_c} \left( \frac{h^2}{2\pi m k_B T_e} \right)^{3/2} \sqrt{\frac{2}{m}} \int_{\varepsilon_{ic}}^{\infty} \sigma_{ic}(\varepsilon) \varepsilon F(\varepsilon - \varepsilon_{ic}) d\varepsilon,$$

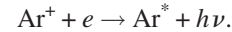
with  $g_e, g_i$ , and  $g_c$  the degeneracies of the electrons, the argon-excited state, and the ionized fundamental state.  $T_e$  is the electron kinetic temperature defined through  $\langle u \rangle = 3/2 k_B T_e$ ,  $\langle u \rangle$  being the mean kinetic energy and  $k_B$  the Boltzmann's constant.

The radiative processes considered are the following.

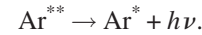
(i) Radiative recombination to the ground state:



(ii) Radiative recombination to an excited state:



(iii) Radiative deexcitation:



The radiative recombination rate coefficients can be expressed as [5]

$$A_{ci} = \sqrt{\frac{2}{m}} \int_0^{\infty} \varepsilon^{1/2} q_{ci}(\varepsilon) f(\varepsilon) d\varepsilon,$$

$q_{ci}$  being the radiative recombination cross section.

Taking into account the rate coefficients previously defined, the collisional balance equation for the excited state  $i$  yields

$$\left. \frac{\partial n_i}{\partial t} \right|_{CR} = \sum_{j \neq i} (K_{ji} n_e + A_{ji}) n_j + K_{ci} n_e^3 + A_{ci} n_e^2 - \left( \sum_{j \neq i} K_{ij} n_e + \sum_{j \neq i} A_{ij} + K_{ic} n_e \right) n_i, \quad (1)$$

whereas the electrons collisional balance is given by

$$\left. \frac{\partial n_e}{\partial t} \right|_{CR} = \sum_j K_{jc} n_j n_e - \sum_j (K_{cj} n_e + A_{cj}) n_e^2. \quad (2)$$

TABLE II. Summary of references for the updated set of argon ground-state cross sections (see text for details).

Number	Configuration	Reference
1	4s[3/2] <sub>2</sub>	Khakoo <i>et al.</i> [9]
2	4s[3/2] <sub>1</sub>	Khakoo <i>et al.</i> [9]
3	4s'[1/2] <sub>0</sub>	Khakoo <i>et al.</i> [9]
4	4s'[1/2] <sub>1</sub>	Khakoo <i>et al.</i> [9]
5-14	4p	Chilton <i>et al.</i> [10]
15	3d+5s	Vlcek [5]
16	3d'+5s'	Vlcek [5]
17-26	5p	Weber <i>et al.</i> [11]
27	4d	Drawin expression [7]
28	6s	Drawin (1967)
29	4d'	Drawin (1967)
31	3s <sup>2</sup> p <sup>5</sup>	Rapp and Englander-Golden [12]

**Electron-impact cross sections and radiative decay probabilities**

The electron-impact cross sections from argon ground state used in this work are summarized in Table II. The experimental data used for the 4s, 4p, and 5p excited configurations have the advantage of describing in detail the low-energy region of the excitation cross section, but one of the main important drawbacks is that the experimental values are limited to energies generally lower than 100 eV. This problem is not present in previous CR models, as they use analytical fits: both Bretagne *et al.* [15] and Vlcek [5] use Drawin expressions for the optically allowed and forbidden transitions whose parameters are chosen in order to fit the low-energy experimental data of Chutjian and Cartwright [13] or Peterson and Allen [14]. In this work, analytical expressions based in those obtained by Bretagne *et al.* [15] are used for the high-energy region with the parameters chosen in order to ensure a smooth fit between the experimental low-energy values and the asymptotic tails.

This cross section set has been validated by comparing with experimental argon transport coefficients and swarm data. One of the main results is that the electron-impact excitation cross sections to the two metastable 4s states (i.e., the 4s[3/2]<sub>2</sub> and the 4s'[1/2]<sub>0</sub> levels) have been rescaled by a factor 0.5 from the experimental values of Khakoo *et al.* [9] in order to ensure a good fit to the experimental data of Tachibana [16]. For the upper levels for which there are no experimental data available, the following Drawin-like expression for optically allowed transitions [7] is used:

$$\sigma(u) = 4\pi a_0 f_{ij} \left( \frac{E_{ion}^H}{\epsilon_{ij}} \right)^2 \frac{(u-1)}{u^2} \ln(1.25u),$$

where  $a_0$  is the Bohr's radius,  $E_{ion}^H$  the atomic hydrogen ionization energy,  $\epsilon_{ij}$  the threshold energy,  $u = \epsilon/\epsilon_{ij}$ , and  $f_{ij}$  the oscillator strength of the optical transition.

Compared with the electron-impact processes from the ground state, the data available for electron impact transitions between excited states are very scarce. From the theo-

retical point of view, the 4s-4p transitions were studied by Hyman in 1978 [17] and 1981 [18] and Kimura *et al.* [19] in 1985. In the first case, both the 4s and 4p excited configurations were considered as lumped levels so that only a total excitation cross section was derived (hereafter referred as block cross section). The results of Kimura *et al.* were obtained under the *j-K* coupling assumption, so that two different values were presented corresponding to the primed and unprimed configurations. Their numerical results were fitted to Drawin's expressions for optically allowed transitions. Another theoretical value for this block cross section was presented by Bretagne *et al.* [4], yielding an excitation cross section close to the theoretical results of Hyman.

In literature there are some argon CR model that divide the 4s and 4p configurations into different sublevels: Vlcek [5] considered the four 4s individual excited states and six effective levels belonging to the 4p configuration. Guimaraes and Bretagne [20], on the other hand, took the ten excited states of this configuration individually, whereas both the models of Bogaerts *et al.* [6] and Bultel *et al.* [7] followed the scheme proposed by Vlcek.

In all cases, the procedure described for determining the individual excitation cross sections was based on ponderating the block excitation cross section  $\sigma_T$  by the oscillator strengths of the radiative transitions between the two levels, so that

$$\sigma_{ij} = f_{ji} \frac{\sigma_T}{\sum_j f_{ji}}. \tag{3}$$

In the model of Guimaraes and Bretagne a value of  $\sigma_T$  close to the theoretical values provided by Hyman and the experimental oscillator strengths obtained by Wiese *et al.* [32] were used. Vlcek [5] followed the same procedure, but using the cross sections obtained by Kimura *et al.* [19].

However, recently some new works have appeared providing theoretical or experimental values for the individual 4s-4p cross sections. In 1996 Boffard *et al.* [21] presented measurements of excitation cross sections from the 4s metastable states to some 4p levels. Piech *et al.* [22] in 1998 also determined experimentally apparent cross sections from the metastable levels to the  $J=3$  excited level of the 4p configuration, providing an estimation of the contribution of radiative cascades of a 20%. In 1999 Bartschat and Zeman [23] presented theoretical calculations that in general fit well the measurements of Piech *et al.* In the same year, Boffard *et al.* [24] published more extensive experimental results, and although only apparent cross sections were presented, in their work the contribution of radiative cascades was estimated to be no more than a 20% of the measured values. The theoretical cross sections of Maloney *et al.* [25] in 2002 agree well with the data of Boffard *et al.*, especially for the more intense transitions.

Using some of these results, Bultel *et al.* [7] presented in 2002 fittings of the Drawin formula to the new cross sections available. However, as has already been mentioned, in their work only six levels belonging to the 4p configuration were considered, and their fittings were limited by the lack of

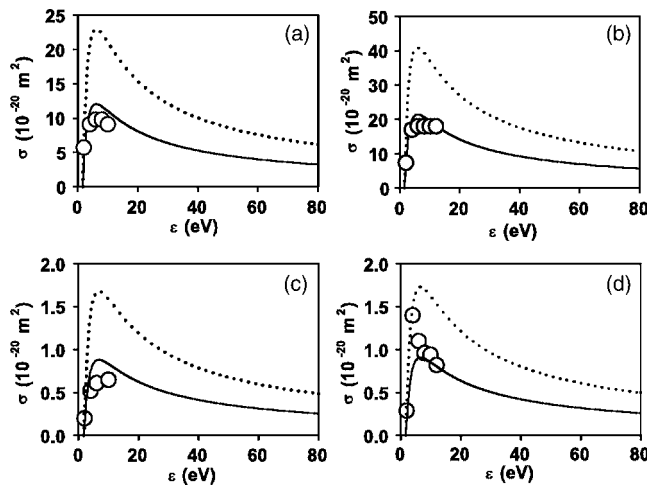


FIG. 1. Electron-impact excitation cross sections for transitions (a)  $4s'[1/2]_0 \rightarrow 4p'[1/2]_1$ , (b)  $4s'[1/2]_0 \rightarrow 4p'[3/2]_1$ , (c)  $4s[3/2]_2 \rightarrow 4p'[1/2]_1$ , and (d)  $4s[3/2]_2 \rightarrow 4p'[3/2]_2$ , as a function of the electron kinetic energy. The experimental results of Boffard *et al.* (open circles) are compared with the cross sections calculated from the block cross sections from Bretagne *et al.* (solid line) and Kimura *et al.* (dotted line).

experimental results for electron-impact excitation cross sections from the  $4s$  radiative states.

In Fig. 1, a comparison between some of the experimental data presented by Boffard *et al.* in 1999 and the individual cross sections obtained through Eq. (3) using the total cross sections provided by Bretagne *et al.* [4] and Kimura *et al.* [19] are presented. The measurements of Boffard *et al.* seem to confirm the existence of a correlation between the intensity of the excitation cross section and the oscillator strength of the radiative decay, especially for the more intense transitions. The use of Eq. (3) is therefore justified. The agreement is clearly better with the block cross section provided by Bretagne *et al.* than in the case of Kimura *et al.* As there is an important lack of data for the excitation cross sections from the  $4s$  radiative states, for the sake of consistency in this work the individual cross sections between levels of the  $4s$  and the  $4p$  configuration have been calculated by means of the block cross sections of Bretagne *et al.* and Eq. (3), due to the fair agreement with the measurements of Boffard *et al.* [24].

No experimental values have been found in literature for transitions between other excited configurations. The cross sections used in the present work are based on the theoretical calculations of block excitation cross sections of Kimura *et al.* [19], using expression (3) for the individual cross sections in optically allowed transitions. In the case of optically forbidden transitions, the results of Kimura *et al.* have been also used.

In spite of their great importance, there are very few experimental results of the excitation exchange by electron impact between excited states belonging to the argon  $4s$  configuration. Both in Vlcek's model [5] and in the later modification of Bogaerts *et al.* [6] the results of Baranov are referenced for the  $4s[3/2]_1 \rightarrow 4s[3/2]_2$  and  $4s'[3/2]_1 \rightarrow 4s'[1/2]_0$  transitions. In these works the values for the

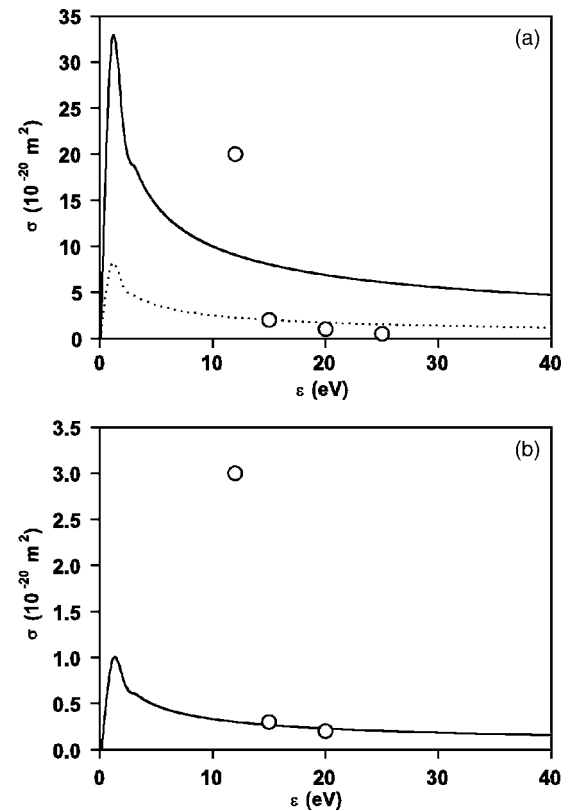


FIG. 2. Electron-impact excitation cross sections for transitions (a)  $4s[3/2]_2 \rightarrow 4s[3/2]_1$  and (b)  $4s[3/2]_2 \rightarrow 4s'[1/2]_0$ , as a function of the electron kinetic energy. The expressions presented by Bogaerts *et al.* (solid line) are compared with the theoretical calculations of Bartschat and Zeman (open circles) and the rescaled Bogaerts cross section in order to fit Bartschat results (dotted line).

other transitions are supposed following the results known for the case of neon.

However, in 1999 Bartschat *et al.* [23] obtained theoretical values of the electron-impact excitation cross sections between the metastable and radiative  $4s$  states. As the results obtained in the same work for the  $4s$ - $4p$  transitions agree well with the experimental measurements of Piech *et al.* [22], the theoretical cross sections of Bartschat and Zeman [23] can be considered good approximations at higher energies of the real cross sections between the  $4s$  excited states. The comparison between the theoretical values of Bartschat and Zeman the expressions provided by Bogaerts *et al.* [6] (see Fig. 2) yields a good agreement except for the case of the  $4s[3/2]_1 \rightarrow 4s[3/2]_2$  transition [Fig. 2(a)], in which one cross section is 4 times greater than the other. In this work, therefore, the expressions presented by Bogaerts *et al.* [6] will be used in  $4s$ - $4s$  transitions except for the  $4s[3/2]_1 \rightarrow 4s[3/2]_2$  cross section, which has been renormalized in order to fit the results of Bartschat and Zeman.

Apart from the  $4s$  transition, hardly any result has been found for excitation exchanges between levels belonging to the same excited configuration. Only in the work of Bultel *et al.* [7] is proposed the use of a general Drawin-shaped cross section for all of them. The influence of these excitation exchanges may be important when determining the popula-

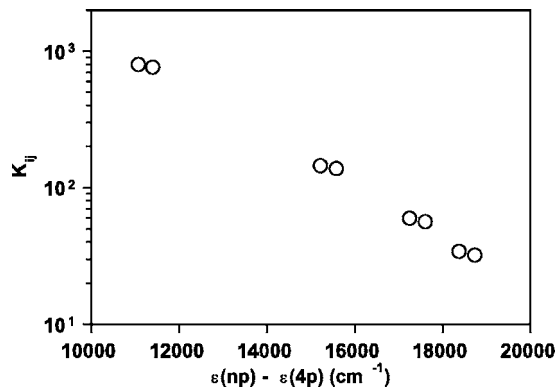


FIG. 3. Threshold energy dependence of the amplitude factors for  $4p$ - $np$  transitions given by Kimura *et al.* (see text for details).

tions of the  $4p$  and  $5p$  transitions, which affect the populations of the  $4s$  levels through radiative decay. For the  $4p$  configuration, Nguyen and Sadeghi [26] studied excitation exchanges driven by atomic impact, whereas Sadeghi [27] provided rate coefficients for the excitation exchange due to the effect of thermal electrons.

In the present work, this kind of transitions are important for the  $4p$  and  $5p$  excited configurations, as in both cases the ten individual levels are considered independently. Therefore, we have used the Drawin's cross-section shape for optically forbidden transitions [7]. The absolute values of the cross sections have been determined by studying the  $4p$ - $np$  and  $5p$ - $np$  cross sections calculated by Kimura *et al.* [19]. Figure 3 shows clear trends of the  $K_{ij}$  coefficients with the transition energy, so that the absolute values have been determined by extrapolating to a zero value of threshold energy.

Compared to ionization from the argon ground state, ionization by electron impact from excited states is not so well studied. The theoretical works commonly cited are those of Ton-That and Flannery [28], Hyman [29], and Vriens and Smeets [30]. In the first of them, the ionization cross section from argon metastable states is theoretically calculated. Hyman in 1979 derived cross sections for the  $4s$  and  $4p$  excited configurations, and in 1980 Vriens and Smeets presented a generic model which has been applied for the case of argon.

In the CR model of Bretagne *et al.* of 1982 [4] a comparison was made between these models and the experimental measurements of Dixon (cited by Bretagne *et al.*) for the ionization from the  $4s$  excited configuration. They also proposed a generic expression for ionization from excited states that fit well the former results. In the model of Guimaraes and Bretagne [20] these cross sections are used. In the CR model of Vlcek [5], a formula proposed by Drawin was chosen, adjusting the coefficients to the results of Hyman [29] for the  $4s$  and  $4p$  excited configurations and using the results of Drawin for the rest of excited levels. These values are also included in later modifications of this model (i.e., Kelkar *et al.* [31], Bogaerts *et al.* [6], or Bultel *et al.* [7]) and are used in the present work.

As for the radiative processes, the experimental measurements of radiative decay probabilities of Wiese *et al.* [32] have been used when possible, as well as the theoretical

values of Lilly [33], Lee and Lu [34], Katsonis and Drawin [35], and Kimura *et al.* [19] for the transitions from the upper excited states.

In the special case of radiative transitions to the argon ground state, the Einstein coefficients  $A_{ij}$  have been modified using escape factors to take into account the possible radiation trapping. These coefficients have been calculated using the theoretical model proposed by Holstein, so that effective Einstein coefficients  $A_{ij}^{ef} = \kappa_{ij} A_{ij}$  are defined, being the  $\kappa_{ij}$  the so-called Holstein's coefficients [36–38].

The treatment of radiative recombination followed in this work relies on the detailed balance principle in order to relate the radiative recombination cross sections to the corresponding photoionization cross sections. Only the recombination to the ground state and the  $4s$  and  $4p$  excited configurations have been taken into account, and in all cases the cross sections provided by Vlcek [5] have been used. However, the influence of this process in the present conditions has turned out to be negligible.

### III. MODEL EQUATIONS

The CR model has been self-consistently solved with the homogeneous electron Boltzmann equation in the two term expansion for a microwave discharge [39]. Under the high-frequency approximation, admitting that  $\omega \gg \kappa v_m$  with  $\omega$  the field excitation frequency and  $\kappa = m/M$ , being  $m$  and  $M$  the electron and argon mass, the time-independent electron Boltzmann equation can be used.

In this work, apart from the electron-neutral and electron-electron elastic collisions and the inelastic collisions from argon ground states, the superelastic processes and the inelastic collisions involving argon excited states are taken into account. The electron-energy distribution function can then be obtained from the equation

$$-\frac{2}{3} \frac{e^2 E^2}{m} \epsilon^{-1/2} \frac{\partial}{\partial \epsilon} \left[ \frac{v_m}{\omega^2 + \nu^2} \epsilon^{3/2} \frac{\partial F}{\partial \epsilon} \right] = S_{0n} + S_{0in} + S_{0sup} + S_{0e}, \quad (4)$$

with the EEDF normalized such that  $\int \epsilon^{1/2} F(\epsilon) d\epsilon = 1$  and  $S_{0n}$  being the term responsible for the electron-argon elastic collisions,  $S_{0e}$  the term of electron-electron collisions, and  $S_{0in}$  and  $S_{0sup}$  those corresponding to the inelastic and superelastic processes. The formulation of these terms is well known and the expressions used can be found elsewhere [40–43].

The discretization presented in 1982 by Bretagne *et al.* [4], based on the previous work of Rockwood [40], has been used. This discretization procedure ensures both particle and energy conservation in the treatment of the electron-electron term. The homogeneous electron Boltzmann equation has been solved coupled to the collisional radiative model for the argon excited states using the electron-impact cross-section set described in Sec. II along with the electron-neutral elastic momentum transfer cross section proposed by Yamabe *et al.* [41]. The inelastic contribution to this cross section has been added using the set presented in this work (Table II).

A low-pressure discharge in a cylindrical configuration has been considered. Among all the argon excited states only

argon metastable levels are affected by radial diffusion due to their longer mean life. For these two states, the balance equation yields

$$\left. \frac{\partial n_m}{\partial t} \right|_{CR} = \frac{D_m}{\Lambda^2},$$

with  $D_m$  the diffusion coefficient for each metastable state given by Sadeghi and  $\Lambda = a/2.4$ , being  $a$  the inner discharge radius. The populations of the radiative excited states are obtained by simply solving the collisional balance

$$\left. \frac{\partial n_i}{\partial t} \right|_{CR} = 0.$$

The CR model and Boltzmann equation have been solved using a semi-implicit relaxation scheme similar to that presented by Morgan and Penetrante [43].

#### IV. RESULTS

The model described in the previous sections has been applied to an argon microwave discharge generated by an electromagnetic field with an excitation frequency of 2.45 GHz in a cylindrical configuration with an inner radius of 1 cm. The model has been solved for a gas temperature of 300 K. The reduced electric field  $E/N$  and ionization degree  $n_e/N$  have been considered as independent variables in order to study the influence of each of them individually. In the calculation of the populations of the excited states the pressure was set to 1 mbar.

In Fig. 4 the EEDF's obtained are presented for three ionization degrees both neglecting [Fig. 4(a)] and considering [Fig. 4(b)] the influence of inelastic and superelastic processes between excited states. When just inelastic processes involving the argon ground state are considered the EEDF tends, as is expected, to a Maxwellian distribution function for higher ionization degrees. However, when the influence of the excited states is taken into account, the EEDF is also affected by the increase of the population of the argon excited states, and both the inelastic and superelastic processes become important for ionization degrees over  $10^{-5}$ . For a value of the reduced field of  $E/N=100$  Td, the increase of the population of the excited states causes the population of the high-energy tail of the EEDF as a consequence of the superelastic processes. At higher ionization degrees the EEDF also tends to a Maxwellian EEDF, but its slope is steeper than in the case of Fig. 4(a), due to the inelastic collisions between excited states, which act as an additional energy-loss term for the free electrons. The evolution of the EEDF with the ionization degree as a consequence of the inelastic and superelastic processes is shown in Fig. 5 for a reduced field  $E/N=100$  Td.

The electron temperature, defined so that  $u_m = 3/2 k_B T_e$ , with  $u_m$  the mean kinetic energy calculated from the electron EEDF, is presented in Fig. 6 both neglecting and considering inelastic and superelastic processes with the excited states. When the contribution of the argon excited states to the EEDF is neglected [Fig. 6(a)], the electron temperature is almost independent of the ionization degree, presenting im-

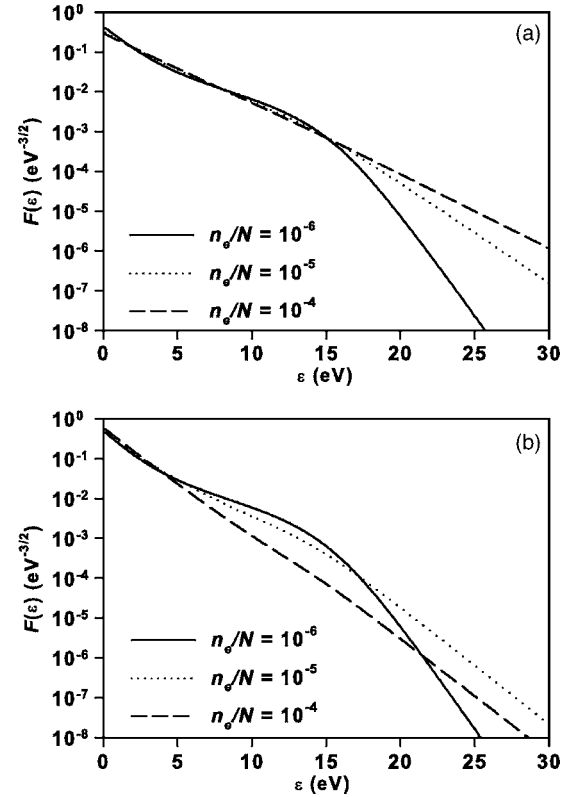


FIG. 4. Electron-energy distribution functions obtained for different ionization degrees at  $E/N=100$  Td: (a) neglecting the contribution of the excited states and (b) full model.

portant variations when increasing the reduced electric field. In Fig. 6(b), on the other hand, the increase of the population of the excited states affects greatly this value, reducing the electron mean energy, especially at high values of  $E/N$ , for ionization degrees over  $10^{-5}$ . Below this limit the influence of inelastic and superelastic processes involving argon excited states is just of second order.

In Fig. 7 the populations of the excited states are shown for an electric field of 100 Td and ionization degrees of  $10^{-5}$  and  $10^{-4}$ : the excited states over the  $4s$  configuration (i.e.,  $i > 4$ ) follow approximately a Boltzmann-like behavior such that

$$n_i = \frac{g_i}{g_0} \exp\left(\frac{-E_i}{k_B T^*}\right),$$

especially for high ionization degrees. One exception is the level  $n=29$ . As its electronic configuration is  $3s^2 p^5 4f$ , the outer electron is weakly coupled to the rest of the levels so that the only important populating pathways are the electron-impact excitations from the  $nd$  configurations.

From the fitting of the excited states over the  $4s$  (with the exception of the  $n=29$  level) to the previous expression it is possible to obtain an argon excitation temperature  $T^*$ . For a ionization degree of  $10^{-4}$  a value of  $T^*=0.9$  eV is obtained. This temperature is lower than the kinetic electron temperature ( $T_e=1.6$  eV) calculated from the EEDF, due to the influence of radiative decays.

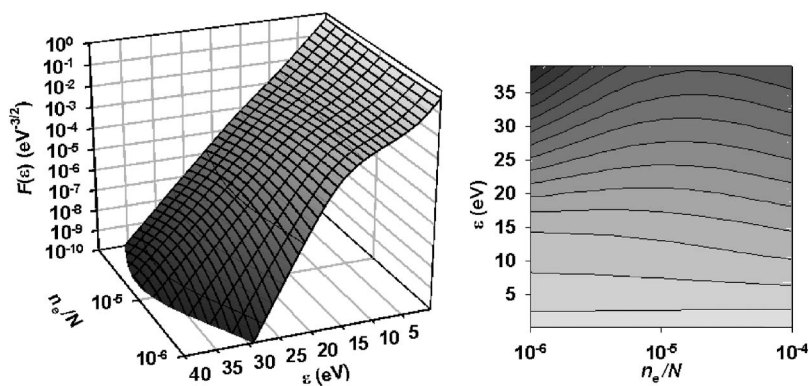


FIG. 5. Electron density influence on the electron-energy distribution function ( $p=1$  mbar,  $T=300$  K,  $E/N=100$  Td).

A comparison of the electron kinetic temperature and the excitation temperature is presented in Fig. 8(a). As the ionization degree increases, the collisional processes become more important and the values of both magnitudes approach each other. The Boltzmann decreases—that is, the quotient between the populations obtained through the collisional radiative model and those predicted by Boltzmann relation for an excitation temperature equal to the electron kinetic temperature—get closer to unity [Fig. 8(b)] as the ionization degree increases as a consequence of the greater influence of the electron collisional deexcitation compared with the radiative decay.

V. DISCUSSION

In the last ten years knowledge of the kinetics of the argon lower excited states has deepened due to the number of new

results of electron-impact excitation cross sections. The advances are also important in the case of the  $4s-4p$  transitions, as now there are experimental data for many electron-impact cross sections involving these two electronic configurations. From the comparison of these experimental data and some of the previous theoretical collisional-radiative models, it has been found that the usual assumption of supposing the intensity of the electron-impact cross section proportional to the oscillator strength of the optical transition is justified.

However, there is still an important lack of data involving either transitions between highly excited states or between levels belonging to the same electron configuration. This lack of data is especially important in the case of the  $4s$  excited configuration, as the main decaying pathway for this states at low pressures is due to excitation interchange with the  $4s$  radiative levels. In this work the values for these cross sections have been chosen taking into account both previous theoretical results and other collisional-radiative models.

The application of the CR model to the calculation of the EEDF using the two-term expansion of the Boltzmann equation shows that the influence of the inelastic processes between excited states leads to a decrease on the electron mean kinetic energy for ionization degrees greater than  $10^{-5}$  compared to the value expected if such transitions are not taken into account. At low fields, this effect becomes less important and the well-known similarity relation  $F(\epsilon) = f(E/N, n_e/N, \omega/N)$  for the electron-energy distribution function remains valid. The introduction of inelastic and superelastic processes in the calculation of the EEDF leads to a

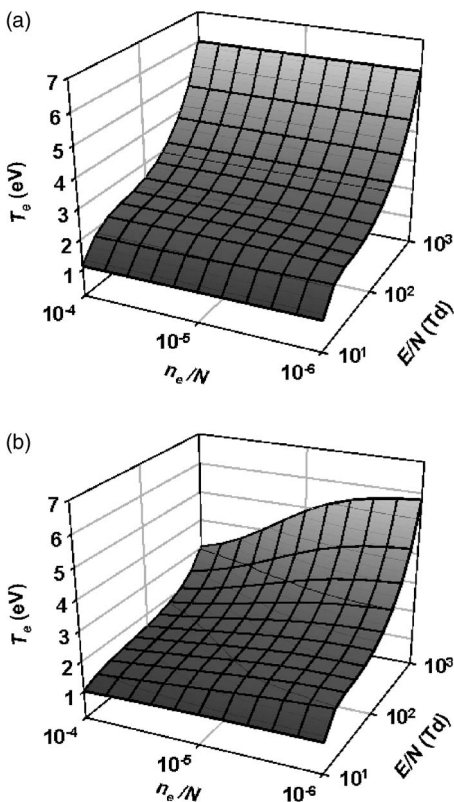


FIG. 6. Effect of the electron density and electric field on the electron kinetic temperature ( $T=300$  K): (a) neglecting the contribution of the excited states and (b) full model.

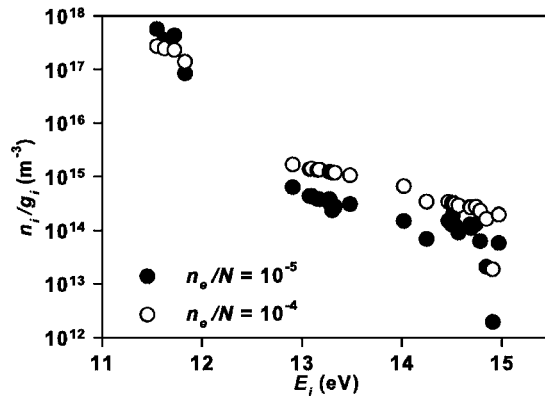


FIG. 7. Populations of argon-excited states for two different ionization degrees:  $n_e/N=10^{-5}$  (solid circles) and  $n_e/N=10^{-4}$  (open circles) ( $T=300$  K,  $E/N=100$  Td).

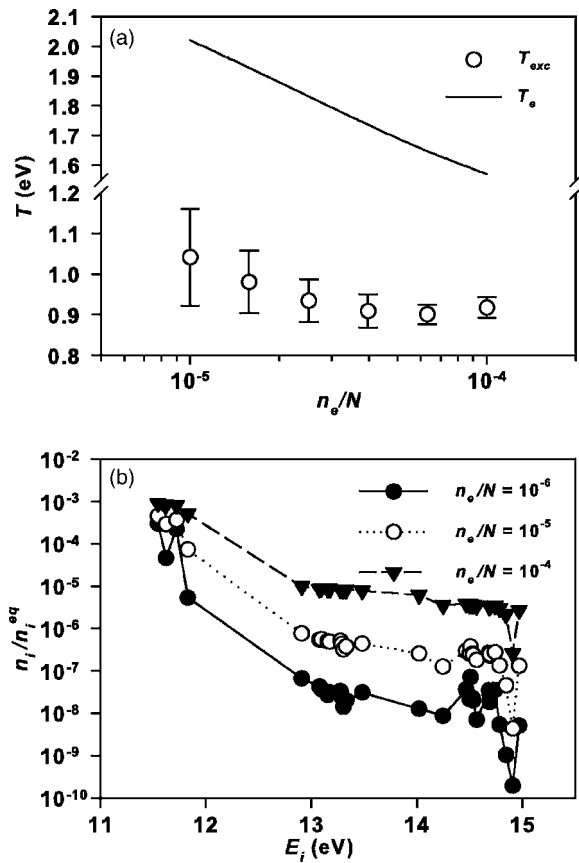


FIG. 8. Influence of the electron density on the populations of the excited states ( $T=300$  K,  $E/N=100$  Td): (a) comparison between the excitation and electron kinetic temperature and (b) Boltzmann decrease (see text for details).

breaking of this relation due to the strong dependence of the reduced densities  $n_i/N$  of the excited states with the gas density  $N$ , a direct consequence of the presence of the radiative processes in the balance equations. In Fig. 9, electron temperatures are presented for constant values of  $E/N$ ,  $n_e/N$ , and  $\omega/N$  at different pressures. If the similarity relation were valid,  $T_e$  would be independent of pressure, and therefore would take a constant value in Fig. 9. However, the influence of the excited states in the EEDF causes a departure from this constant value, so that  $T_e$  decreases when increasing this parameter. In the low-pressure limit, the influence of the excited states on the EEDF turns out to be negligible.

As is expected, the populations of the excited states vary greatly with the electric field and ionization degree. At lower electron densities, where the excitation exchanges are not important, the populations of the excited states are strongly affected by the excitation cross sections from the ground state and the radiative decays. However, as the ionization

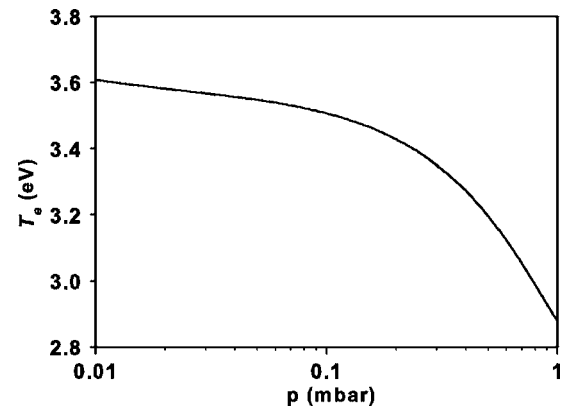


FIG. 9. Influence of pressure on the electron temperature ( $T=300$  K,  $E/N=100$  Td,  $n_e/N=10^{-5}$ ,  $\omega/N=2 \times 10^{-13}$  s $^{-1}$  m $^3$ ).

degree increases, the populations of the excited states tend to a relation consistent with a Boltzmann profile, so that an excitation temperature can be defined. Such an excitation temperature can be experimentally determined from optical emission spectroscopy (OES) measurements [44], but contrary to what it is generally assumed at atmospheric pressure, at low pressure its value is lower than the electron kinetic temperature due to the influence of the radiative decay. This means that from the experimental point of view the determination of  $T_e$  based on OES measurement that is normally used at atmospheric pressure can not be applied to lower pressures.

## VI. CONCLUSIONS

In this work an argon collisional-radiative model has been developed taking into account the new values of electron-impact cross sections that have been recently published. With these model the electron-energy distribution function has been calculated using a two-term expansion of the Boltzmann equation considering the influence of both inelastic and superelastic collisions. These processes have a greater influence at high ionization degrees and electric field values, becoming an important energy-loss term at pressures of 1 mbar, and therefore should be considered when modeling argon discharges at such pressures. When increasing the ionization degree the populations of the excited states are related by a Boltzmann-like expression, but the excitation temperature that can be derived is lower than the electron temperature, contrary to what it is usually admitted at atmospheric pressure.

## ACKNOWLEDGMENTS

This research was partially supported by Grant Nos. MAT2001-2820 and PPQ2001-3108 and the Acci3n Integrada HP02-102 from the Direcci3n General de Investigaci3n Científica y T3cnica (Spain).



- [1] A. Barranco, J. Cotrino, F. Yubero, J. P. Espinós, J. Benítez, C. Clerc, and A. R. González-Elipe, *Thin Solid Films* **401**, 150 (2001).
- [2] M. Baeva, A. Pott, and J. Uhlenbusch, *Plasma Sources Sci. Technol.* **11**, 135 (2002).
- [3] M. Laroussi and F. Lerpold, *Int. J. Mass Spectrom. Ion Processes* **233**, 81 (1998).
- [4] J. Bretagne, G. Callede, M. Legentil, and V. Puech, *J. Phys. D* **19**, 761 (1986).
- [5] J. Vlcek, *J. Phys. D* **22**, 623, (1989).
- [6] A. Bogaerts, R. Gijbels, and J. Vlcek, *J. Appl. Phys.* **84**, 121 (1998).
- [7] A. Bultel, B. van Ootegem, A. Bourdon, and P. Vervisch, *Phys. Rev. E* **65**, 046406 (2002).
- [8] A. Yanguas-Gil, J. Cotrino, and A. R. González-Elipe, *Phys. Plasmas* **11**, 5497 (2004).
- [9] M. A. Khakoo, P. Vandeventer, J. G. Childers, I. Kanik, C. J. Fontes, K. Bartschat, V. Zeman, D. H. Madison, S. Saxena, R. Srivastava, and A. D. Stauffer, *J. Phys. B* **37**, 247 (2004).
- [10] J. E. Chilton, J. B. Boffard, R. S. Schappe, and C. C. Lin, *Phys. Rev. A* **57**, 267 (1998).
- [11] T. Weber, J. B. Boffard, and C. C. Lin, *Phys. Rev. A* **68**, 032719 (2003).
- [12] D. Rapp and P. Englander-Golden, *J. Chem. Phys.* **83**, 1464 (1965).
- [13] A. Chutjian and D. C. Cartwright, *Phys. Rev. A* **23**, 2178 (1981).
- [14] L. R. Peterson and J. E. Allen, Jr., *J. Chem. Phys.* **56**, 6068 (1972).
- [15] J. Bretagne, J. Godart, and V. Puech, *J. Phys. D* **15**, 2205 (1982).
- [16] K. Tachibana, *Phys. Rev. A* **34**, 1007 (1986).
- [17] H. A. Hyman, *Phys. Rev. A* **18**, 441 (1978).
- [18] H. A. Hyman, *Phys. Rev. A* **24**, 1094 (1981).
- [19] A. Kimura, H. Kobayashi, M. Nishida, and P. Valentin, *J. Quant. Spectrosc. Radiat. Transf.* **34**, 189 (1985).
- [20] F. Guimaraes and J. Bretagne, *Plasma Sources Sci. Technol.* **2**, 127 (1993).
- [21] J. B. Boffard, G. A. Piech, M. F. Gehrke, M. E. Lagus, L. W. Anderson, and C. C. Lin, *J. Phys. B* **29**, L795 (1996).
- [22] G. A. Piech, J. B. Boffard, M. F. Gehrke, L. W. Anderson, and C. C. Lin, *Phys. Rev. Lett.* **81**, 309 (1998).
- [23] K. Bartschat and V. Zeman, *Phys. Rev. A* **59**, R2552 (1999).
- [24] J. B. Boffard, G. A. Piech, M. F. Gehrke, L. W. Anderson, and C. C. Lin, *Phys. Rev. A* **59**, 2749 (1999).
- [25] C. M. Maloney, J. L. Peacher, K. Bartschat, and D. H. Madison, *Phys. Rev. A* **61**, 022701 (2000).
- [26] T. D. Nguyen and N. Sadeghi, *Phys. Rev. A* **18**, 1388 (1978).
- [27] N. Sadeghi, Ph.D. thesis, University of Grenoble, 1974.
- [28] D. Ton-That and M. R. Flannery, *Phys. Rev. A* **15**, 517 (1977).
- [29] H. A. Hyman, *Phys. Rev. A* **20**, 855 (1979).
- [30] L. Vriens and A. H. M. Smeets, *Phys. Rev. A* **22**, 940 (1980).
- [31] U. M. Kelkar, M. H. Gordon, L. A. Roe, and Y. Li, *J. Vac. Sci. Technol. A* **17**, 125 (1999).
- [32] W. L. Wiese, J. W. Brault, K. Danzmann, V. Helbig, and M. Kock, *Phys. Rev. A* **39**, 2461 (1989).
- [33] R. A. Lilly, *J. Opt. Soc. Am.* **66**, 245 (1976).
- [34] C. M. Lee and K. T. Lu, *Phys. Rev. A* **8**, 1241 (1973).
- [35] K. Katsonis and H. W. Drawin, *J. Quant. Spectrosc. Radiat. Transf.* **23**, 1 (1980).
- [36] T. Holstein, *Phys. Rev.* **72**, 1212 (1947).
- [37] T. Holstein, *Phys. Rev.* **83**, 1159 (1951).
- [38] P. J. Walsh, *Phys. Rev.* **116**, 511 (1959).
- [39] V. E. Golant, A. P. Zhilinsky, I. E. Sakharov, and S. C. Brown, *Fundamentals of Plasma Physics* (Wiley, New York, 1980).
- [40] S. D. Rockwood, *Phys. Rev. A* **8**, 2348 (1973).
- [41] C. Yamabe, S. J. Buckman, and A. V. Phelps, *Phys. Rev. A* **27**, 1345 (1983).
- [42] U. Kortshagen, H. Schlter, and A. Shivarova, *J. Phys. D* **24**, 1751 (1991).
- [43] W. L. Morgan and B. M. Penetrante, *Comput. Phys. Commun.* **58**, 127 (1990).
- [44] M. C. García, A. Rodero, A. Sola, and A. Gamero, *Spectrochim. Acta, Part B* **55**, 1733 (2000).